Robot-Assisted Endodontic Treatment

Yi-Chan Li

Advisor: Cheng-Wei Chen

Graduate Institute of Electronics Engineering

National Taiwan University

Taipei, Taiwan

June 2021

Abstract

Contents

List of Figures

List of Tables

Chapter 1

Introduction

In this chapter, the procedure of the endodontic treatment, so called the root canal treatment, is introduced.

1.1 Motivation

(Introduce the procedure of the endodontic treatment- Open$\longrightarrow$Clean$\longrightarrow$Fill)

1.2 Previous Work and Problem Definition

(Briefly mention some dental robots)
(Focus on cleaning procedure)
(Two problem definition: prevent breakage of file, clean thoroughly)

1.3 The Proposed Method

(Move to the infected teeth$\longrightarrow$Root canal searching$\longrightarrow$Repetitive drilling$\longrightarrow$Apex Detection)
(Challenges: root canal is small, risk of file breakage) (Solutions: 1. Build a robot;2. Force-guided alignment; 3. Control the file rotation speed)

1.4 Main Contributions of the Thesis

1. Integrate a 6-DoF robotic manipulator with 6-DoF F/T sensor for performing endodontic treatment.

2. Develop a framework for robot alignment regarding the position and orientation of root canal.

3. Protect the endodontic file from fracturing by controlling file rotation speed.

Endodontic therapy, also known as root canal treatment, is performed to prevent a tooth from being infected. According to American association of endodontists, more than 15 million root canal treatments are performed every year [1] . Although this therapy had been so prevalent, the outcome largely depends on the clinician's experience and expertise. Instruments fracture and perforation are two problems that commonly occur during the therapy. Removal of broken files is both technically difficult and therefore it is important to reduce the probability of fracture [2] . In addition to these problems, root canal treatment also requires repeatedly drilling in order to clean the canal thoroughly (Fig. 1, "Drilling Root Canal" step). This repetitive action of root canal treatment is tedious and time-consuming. Therefore, we designed an automatic endodontic robot to improve the time-efficiency and to reduce the occurrence of instrument fracture in endodontic surgery. There is one robotic system that is designed to perform endodontic therapy. In Intelligent Micro Robot Development for Minimum Invasive Endodontic Treatment [3] , they proposed a micro robot performing root canal treatment with the assistance of 3D computer model system. It is designed to accomplish endodontic therapy with path planned according to the 3D model. However, the problem of instruments fracture still remains. In this paper, a torque monitoring method is proposed. The main causes of fractured files are torsional fracture and flexural fatigue, account for 55.7% and 44.3% separately [5]. Therefore, we use current feedback to keep track of the torque which the file is bearing during the endodontic treatment. This torque monitoring system is implemented on an endodontic robot prototype we

built. We primarily focus on the cleaning and shaping step since it's the key step to a successful root canal treatment. With the robot prototype and torque monitoring system, the possibility of instrument fracture can be reduced. Besides, the repetitive action during the drilling step can be performed by the robot.

1.5 Organization of the Thesis

Chapter 2

State-of-the-Art

(Elaborate more details of NCTU paper, YOMI and even other dental robots)

(Why not Image processing and why force feedback?)

Chapter 3

Design and Analysis of the Dental Surgical Robot - DentiBot

3.1 Requirement and Specification

(Payload, resolution and workspace)

(Why not RCM mechanism)

3.2 Design of the DentiBot

As discussed in previous section, we have to select suitable devices according to those requirements. First, We choose Meca500 manufactured by Mecadamic Inc. as our 6 DOF robot arm. Its feature is high repeatability (precision: 5 μm) and it is equipped with zero-backlash speed reducers. In addition, it is compact and portable for laboratory investigation. Second, Mini40 manufactured by ATI Inc. is the corresponding F/T sensor with three force and three torque detections. As for the end effector, we modify a existing dental handpiece which equips a tool change mechanism. The modified handpiece weights around 139 grams. We also design adapters so as to assemble these devices.

DentiBot has seven degree of freedom. 6 DOF is come from Meca500, and the

other DOF is owing to our modified handpiece. The rotation of root canal file is driven by a servo motor whose maximum rotation speed is more than 600 rpm.

3.3 Kinematics Analysis

The purpose of this section and section 3.4 is to serve as a tutorial and provide some important approaches when combining a robot arm and an end effector. We derive the forward and inverse kinematics in section 3.3.2 and describe Jacobian matrix in section 3.3.3.

3.3.1 Coordinate Definition

In Fig 3.1 , we define frame$\{0\}$ to frame$\{6\}$ which represent each frame of axis of the Meca500, frame$\{S\}$ which represent the frame of the ATI-mini40 and frame$\{H\}$ which represent the frame of the handpiece.

3.3.2 Forward and Inverse Kinematics

Table 3.1: Denavit-Hartenberg parameters of Meca500

i (link number)	α_{i-1} (deg)	a_{i-1} (mm)	θ_i (deg)	d_i (mm)
1	0	0	θ_1	135
2	-90	0	θ_2	0
3	0	135	θ_3	0
4	-90	38	θ_4	120
5	90	0	θ_5	0
6	-90	0	θ_6	70

Denavit-Hartenberg parameters are shown as Table 3.1. Then, the forward kinematics of Meca500 is derived as

$$ {}^{0}_{6}\mathbf{T} = {}^{0}_{1}\mathbf{T} \cdot {}^{1}_{2}\mathbf{T} \cdot {}^{2}_{3}\mathbf{T} \cdot {}^{3}_{4}\mathbf{T} \cdot {}^{4}_{5}\mathbf{T} \cdot {}^{5}_{6}\mathbf{T} = \begin{bmatrix} {}^{0}_{6}\mathbf{R} & {}^{0}\boldsymbol{p}_{6\text{org}} \\ 0 & 1 \end{bmatrix} $$

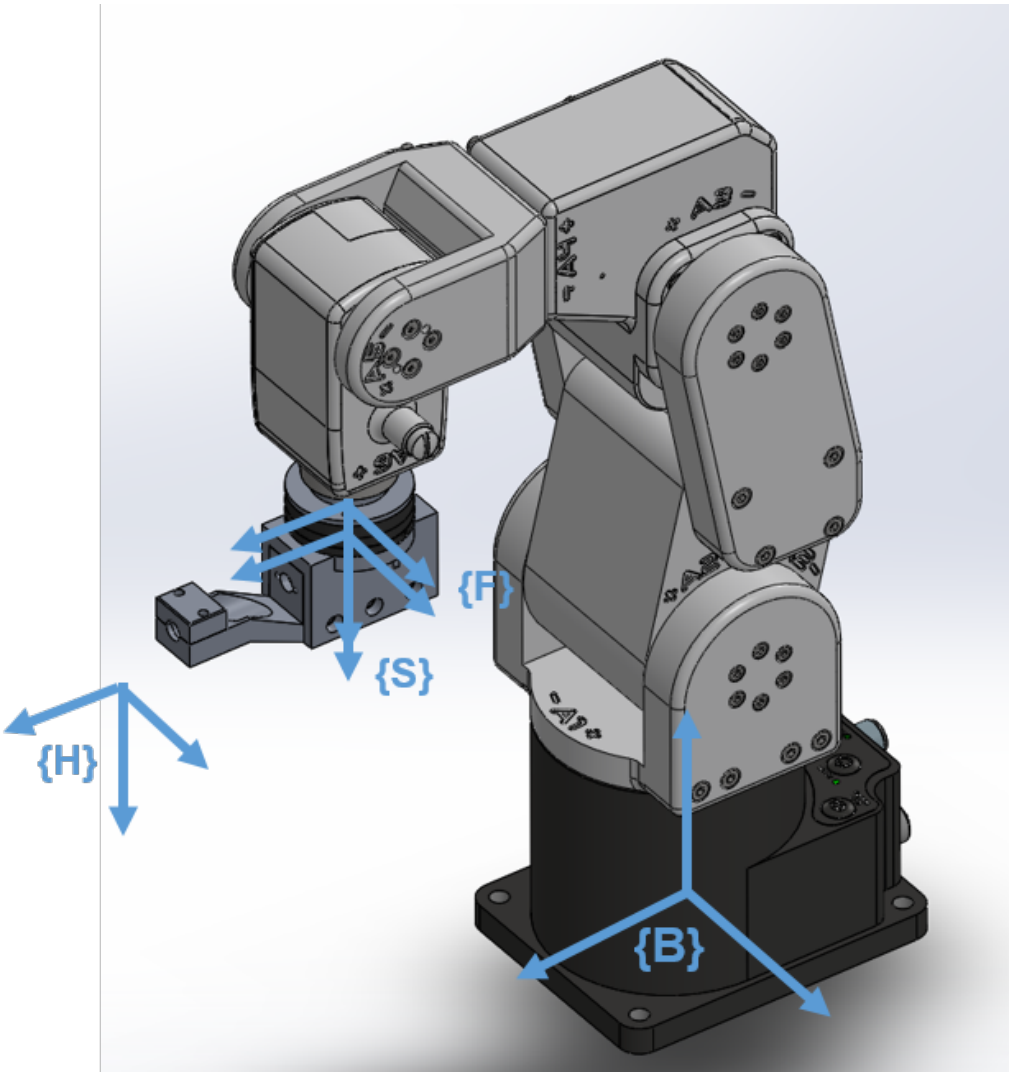

Figure 3.1: Coordinate Definition

where ${}^{0}_{6}\mathbf{R}$ is the rotation matrix from frame$\{6\}$ to frame$\{0\}$, ${}^{0}\boldsymbol{p}_{6\text{org}}$ is the origin of the frame$\{6\}$ observed from frame$\{0\}$.
All detailed indexes of ${}^{0}_{6}\mathbf{T}$ are shown as Appendix 8.1

3.3.3 Jacobian matrix

Here we will derive geometric Jacobian based on frame$\{0\}$, geometric Jacobian based on frame$\{6\}$ and analytical Jacobian.
The difference between geometric Jacobian and analytical Jacobian is the angular velocities they considered. The angular velocities Geometric Jacobian considers is relevant to the axis angles (θ_x,θ_y,θ_z). In contrast, it is related to the orientation (α,β,γ) of the end effector.

Geometric Jacobian Based on Frame{0}

Before proceeding to examine the geometric Jacobian matrix, it will be necessary to find the relationship between the position and joints' angles and the relationship between the axis angle and the joints' angles.
On the basis of the translation matrix in Equation 3.3.2, we obtain the relationship between the position and joints' angles.

$$ {}^{0}\boldsymbol{p}_{6\text{org}} = \begin{bmatrix} x \\ y \\ z \end{bmatrix} = \begin{bmatrix} x(\theta_1, \theta_2, \cdots, \theta_6) \\ y(\theta_1, \theta_2, \cdots, \theta_6) \\ z(\theta_1, \theta_2, \cdots, \theta_6) \end{bmatrix} \tag{3.1} $$

Moreover, we explain the relationship between the axis angle and joints' angles.

$$ \begin{bmatrix} \theta_x \\ \theta_y \\ \theta_z \end{bmatrix} = {}^{0}_{1}\mathbf{R} \begin{bmatrix} 0 \\ 0 \\ \theta_1 \end{bmatrix} + {}^{0}_{2}\mathbf{R} \begin{bmatrix} 0 \\ 0 \\ \theta_2 \end{bmatrix} + {}^{0}_{3}\mathbf{R} \begin{bmatrix} 0 \\ 0 \\ \theta_3 \end{bmatrix} + {}^{0}_{4}\mathbf{R} \begin{bmatrix} 0 \\ 0 \\ \theta_4 \end{bmatrix} + {}^{0}_{5}\mathbf{R} \begin{bmatrix} 0 \\ 0 \\ \theta_5 \end{bmatrix} + {}^{0}_{6}\mathbf{R} \begin{bmatrix} 0 \\ 0 \\ \theta_6 \end{bmatrix} \tag{3.2} $$

We can differentiate Equation 3.3.3 and 3.3.3 to obtain Jacobian matrices.

$$\boldsymbol{v} = \begin{bmatrix} \dot{x} \\ \dot{y} \\ \dot{z} \end{bmatrix} = \mathbf{J_{gv}} \cdot \dot{\boldsymbol{\theta}}, \ \boldsymbol{w} = \begin{bmatrix} \dot{\theta}_x \\ \dot{\theta}_y \\ \dot{\theta}_z \end{bmatrix} = \mathbf{J_{gw}} \cdot \dot{\boldsymbol{\theta}} \tag{3.3}$$

where

$$\mathbf{J_{gv}} = \begin{bmatrix} \frac{\partial x}{\partial \theta_1} & \frac{\partial x}{\partial \theta_2} & \cdots & \frac{\partial x}{\partial \theta_6} \\ \frac{\partial y}{\partial \theta_1} & \frac{\partial y}{\partial \theta_2} & \cdots & \frac{\partial y}{\partial \theta_6} \\ \frac{\partial z}{\partial \theta_1} & \frac{\partial z}{\partial \theta_2} & \cdots & \frac{\partial z}{\partial \theta_6} \end{bmatrix}, \ \mathbf{J_{gw}} = \begin{bmatrix} \frac{\partial \theta_x}{\partial \theta_1} & \frac{\partial \theta_x}{\partial \theta_2} & \cdots & \frac{\partial \theta_x}{\partial \theta_6} \\ \frac{\partial \theta_y}{\partial \theta_1} & \frac{\partial \theta_y}{\partial \theta_2} & \cdots & \frac{\partial \theta_y}{\partial \theta_6} \\ \frac{\partial \theta_z}{\partial \theta_1} & \frac{\partial \theta_z}{\partial \theta_2} & \cdots & \frac{\partial \theta_z}{\partial \theta_6} \end{bmatrix}, \ \dot{\boldsymbol{\theta}} = \begin{bmatrix} \dot{\theta}_1 \\ \dot{\theta}_2 \\ \dot{\theta}_3 \\ \dot{\theta}_4 \\ \dot{\theta}_5 \\ \dot{\theta}_6 \end{bmatrix}$$

As a result, the geometric Jacobian matrix based on frame0 ${}^{\mathbf{0}}\mathbf{J_g}$ is derived as

$$\begin{bmatrix} \dot{x} \\ \dot{y} \\ \dot{z} \\ \dot{\theta}_x \\ \dot{\theta}_y \\ \dot{\theta}_z \end{bmatrix} = {}^{\mathbf{0}}\mathbf{J_g} \cdot \begin{bmatrix} \dot{\theta}_1 \\ \dot{\theta}_2 \\ \dot{\theta}_3 \\ \dot{\theta}_4 \\ \dot{\theta}_5 \\ \dot{\theta}_6 \end{bmatrix} \tag{3.4}$$

There is a further derivation. In terms of the Jacobian matrix, we can derive the other property.

$$\boldsymbol{\tau} = {}^{\mathbf{0}}\mathbf{J}_{\mathbf{g}}^{\top} \cdot \boldsymbol{f} \quad \Leftrightarrow \quad \begin{bmatrix} \tau_{\theta_1} \\ \tau_{\theta_2} \\ \tau_{\theta_3} \\ \tau_{\theta_4} \\ \tau_{\theta_5} \\ \tau_{\theta_6} \end{bmatrix} = {}^{\mathbf{0}}\mathbf{J}_{\mathbf{g}}^{\top} \cdot \begin{bmatrix} f_x \\ f_y \\ f_z \\ \tau_x \\ \tau_y \\ \tau_z \end{bmatrix} \tag{3.5}$$

where $\boldsymbol{\tau}$ is the vector of joints' torques and $\boldsymbol{f}$ is the vector composed of inertial forces and torques of the robot arm.

Geometric Jacobian Based on Frame{6}

Why we need geometric Jacobian based on frame$\{6\}$ is that in section 4.3.1 we will use admittance control and it will use F/T sensor mounted on frame$\{6\}$ instead of frame$\{0\}$. First, we start from Equation 3.3.3

$$\begin{bmatrix} \dot{x} \\ \dot{y} \\ \dot{z} \\ \dot{\theta}_x \\ \dot{\theta}_y \\ \dot{\theta}_z \end{bmatrix}_{\{0\}} = {}^{\mathbf{0}}\mathbf{J_g} \cdot \begin{bmatrix} \dot{\theta}_1 \\ \dot{\theta}_2 \\ \dot{\theta}_3 \\ \dot{\theta}_4 \\ \dot{\theta}_5 \\ \dot{\theta}_6 \end{bmatrix} \tag{3.6}$$

Then, left-multiply a matrix.

$$\begin{bmatrix} {}^0_6\mathbf{R} & 0_{3\times3} \\ 0_{3\times3} & {}^0_6\mathbf{R} \end{bmatrix} \begin{bmatrix} \dot{x} \\ \dot{y} \\ \dot{z} \\ \dot{\theta}_x \\ \dot{\theta}_y \\ \dot{\theta}_z \end{bmatrix}_{\{0\}} = \begin{bmatrix} {}^0_6\mathbf{R} & 0_{3\times3} \\ 0_{3\times3} & {}^0_6\mathbf{R} \end{bmatrix} {}^{\mathbf{0}}\mathbf{J_g} \cdot \begin{bmatrix} \dot{\theta}_1 \\ \dot{\theta}_2 \\ \dot{\theta}_3 \\ \dot{\theta}_4 \\ \dot{\theta}_5 \\ \dot{\theta}_6 \end{bmatrix} \tag{3.7}$$

According to the transformation coordinate relationship between frame$\{0\}$ and frame$\{6\}$,

$$\begin{bmatrix} \dot{x} \\ \dot{y} \\ \dot{z} \\ \dot{\theta}_x \\ \dot{\theta}_y \\ \dot{\theta}_z \end{bmatrix}_{\{6\}} = \begin{bmatrix} {}^0_6\mathbf{R} & 0_{3\times3} \\ 0_{3\times3} & {}^0_6\mathbf{R} \end{bmatrix} \begin{bmatrix} \dot{x} \\ \dot{y} \\ \dot{z} \\ \dot{\theta}_x \\ \dot{\theta}_y \\ \dot{\theta}_z \end{bmatrix}_{\{0\}} \tag{3.8}$$

substitute it into Eq 3.3.3, we can observe that the final equation is

$${}^{\mathbf{6}}\mathbf{J_g} = \begin{bmatrix} {}^0_6\mathbf{R} & 0_{3\times3} \\ 0_{3\times3} & {}^0_6\mathbf{R} \end{bmatrix} \cdot {}^{\mathbf{0}}\mathbf{J_g} \tag{3.9}$$

Analytical Jacobian

The linear velocity of analytical Jacobian and of geometric Jacobian is the same shown in Eq 3.3.3. However, as for angular velocity, analytical Jacobian takes the the orientation (α,β,γ) of the end effector as consideration. First of all, we explain the relationship between the axis angle and the orientation of the end effector as following.

$$\begin{aligned}\begin{bmatrix}\theta_x\\ \theta_y\\ \theta_z\end{bmatrix} &= \begin{bmatrix}\alpha\\ 0\\ 0\end{bmatrix} + R_x(\alpha)\begin{bmatrix}0\\ \beta\\ 0\end{bmatrix} + R_x(\alpha)R_y(\beta)\begin{bmatrix}0\\ 0\\ \gamma\end{bmatrix}\\ &= \begin{bmatrix}1 & 0 & S_\beta\\ 0 & C_\alpha & -S_\alpha C_\beta\\ 0 & S_\alpha & C_\alpha C_\beta\end{bmatrix}\begin{bmatrix}\alpha\\ \beta\\ \gamma\end{bmatrix}\end{aligned} \tag{3.10}$$

Then, utilize this generalized vector to get its Jacobian matrix $\mathbf{J_{we}}$.

$$\begin{bmatrix}\dot{\theta}_x\\ \dot{\theta}_y\\ \dot{\theta}_z\end{bmatrix} = \mathbf{J_{we}} \cdot \begin{bmatrix}\dot{\alpha}\\ \dot{\beta}\\ \dot{\gamma}\end{bmatrix} \tag{3.11}$$

where

$$\mathbf{J_{we}} = \begin{bmatrix}1 & \gamma C_\beta & S_\beta\\ -\beta S_\alpha - \gamma C_\alpha C_\beta & C_\alpha + \gamma S_\alpha S_\beta & -C_\beta S_\alpha\\ \beta C_\alpha - \gamma C_\beta S_\alpha & S_\alpha - \gamma C_\alpha S_\beta & C_\alpha C_\beta\end{bmatrix} \tag{3.12}$$

Therefore,

$$\begin{bmatrix}\dot{x}\\ \dot{y}\\ \dot{z}\\ \dot{\theta}_x\\ \dot{\theta}_y\\ \dot{\theta}_z\end{bmatrix} = \begin{bmatrix}\mathbf{I}_{3\times3} & 0_{3\times3}\\ 0_{3\times3} & \mathbf{J_{we}}\end{bmatrix}\begin{bmatrix}\dot{x}\\ \dot{y}\\ \dot{z}\\ \dot{\alpha}\\ \dot{\beta}\\ \dot{\gamma}\end{bmatrix} \tag{3.13}$$

Finally, we obtain the relationship between geometric and analytical Jacobian.

$$\mathbf{J_g} = \begin{bmatrix} \mathbf{I}_{3\times3} & 0_{3\times3} \\ 0_{3\times3} & \mathbf{J_{we}} \end{bmatrix} \mathbf{J_a},\ \mathbf{J_g} = \begin{bmatrix} \mathbf{I}_{3\times3} & 0_{3\times3} \\ 0_{3\times3} & \mathbf{J_{we}^{-1}} \end{bmatrix} \mathbf{J_a} \tag{3.14}$$

3.4 Reference Frame Changing of the Robot Arm

So far, with forward and inverse kinematics the robot arm can translate and rotate around frame$\{6\}$. However the origin of the frame$\{6\}$ is not considered to be an operating point. Because the F/T sensor and a detachable end effector will be both mounted on the wrist, the position of the tool tip is exactly what we want. That means we should let the robot arm know how to translate and rotate in frame$\{\mathrm{T}\}$ instead of frame$\{6\}$. If we have translation and rotation information of the tool tip, there is an easy way to directly give these above information to the robot arm. SetTRF (x,y,z,α,β,γ) is the command of the robot arm, whose (x,y,z) is translation vector and (α,β,γ) is rotation vector in representation of Euler angle .
In order to obtain translation and rotation vector, we respectively introduce Tool Center Point in section 3.4.1 to find the translation vector and propose an approach in section 3.4.2 to find the rotation vector.

3.4.1 Tool Center Point

Tool Center Point (TCP) is a critical problem for robot arm control. In previous section, we have calculated the forward and inverse kinematics of the robot arm. By Calculating kinematics we can keep track of the origin of the frame$\{6\}$, which is observed from the base frame. The robot arm has capability to translate and rotate with the origin of the frame$\{6\}$. These above motions is like a remote center motion (RCM). We should find the position of the tool tip and make it be a RCM point. Nevertheless, it's not efficient to recalculate the transformation matrix via mechanism dimension when changing an end effector or a tool (root canal reamer). To overcome this problem, we demonstrate four-points method to obtain the

position of the tool tip which is also the translation vector.

From Fig 3.1, we can obtain the following transformation matrix,

$$ {}^{\mathrm{B}}_{\mathrm{H}}\mathbf{T} = {}^{\mathrm{B}}_{\mathrm{F}}\mathbf{T} \cdot {}^{\mathrm{F}}_{\mathrm{H}}\mathbf{T} \tag{3.15} $$

and it can be rewritten as

$$ \begin{aligned} \begin{bmatrix} {}^{\mathrm{B}}_{\mathrm{H}}\mathbf{R} & {}^{\mathrm{B}}\boldsymbol{p}_{\mathrm{H_{org}}} \\ 0 & 1 \end{bmatrix} &= \begin{bmatrix} {}^{\mathrm{B}}_{\mathrm{F}}\mathbf{R} & {}^{\mathrm{B}}\boldsymbol{p}_{\mathrm{F_{org}}} \\ 0 & 1 \end{bmatrix} \begin{bmatrix} {}^{\mathrm{F}}_{\mathrm{H}}\mathbf{R} & {}^{\mathrm{F}}\boldsymbol{p}_{\mathrm{H_{org}}} \\ 0 & 1 \end{bmatrix} \\ &= \begin{bmatrix} {}^{\mathrm{B}}_{\mathrm{F}}\mathbf{R} \cdot {}^{\mathrm{F}}_{\mathrm{H}}\mathbf{R} & {}^{\mathrm{B}}_{\mathrm{F}}\mathbf{R} \cdot {}^{\mathrm{F}}\boldsymbol{p}_{\mathrm{H_{org}}} + {}^{\mathrm{B}}\boldsymbol{p}_{\mathrm{F_{org}}} \\ 0 & 1 \end{bmatrix} \end{aligned} \tag{3.16} $$

Therefore, we get a crucial equation:

$$ {}^{\mathrm{B}}\boldsymbol{p}_{\mathrm{H_{org}}} = {}^{\mathrm{B}}_{\mathrm{F}}\mathbf{R} \cdot {}^{\mathrm{F}}\boldsymbol{p}_{\mathrm{H_{org}}} + {}^{\mathrm{B}}\boldsymbol{p}_{\mathrm{F_{org}}} \tag{3.17} $$

Now, we can move the tool tip to a fixed point with four different pose (position and orientation). Then, we will get four different rotation matrix and vectors in real time.

$$ \begin{aligned} {}^{\mathrm{B}}\boldsymbol{p}_{\mathrm{H_{org}}} &= {}^{\mathrm{B}}_{\mathrm{F}}\mathbf{R}^{1} \cdot {}^{\mathrm{F}}\boldsymbol{p}_{\mathrm{H_{org}}} + {}^{\mathrm{B}}\boldsymbol{p}^{1}_{\mathrm{F_{org}}} \\ &= {}^{\mathrm{B}}_{\mathrm{F}}\mathbf{R}^{2} \cdot {}^{\mathrm{F}}\boldsymbol{p}_{\mathrm{H_{org}}} + {}^{\mathrm{B}}\boldsymbol{p}^{2}_{\mathrm{F_{org}}} \\ &= {}^{\mathrm{B}}_{\mathrm{F}}\mathbf{R}^{3} \cdot {}^{\mathrm{F}}\boldsymbol{p}_{\mathrm{H_{org}}} + {}^{\mathrm{B}}\boldsymbol{p}^{3}_{\mathrm{F_{org}}} \\ &= {}^{\mathrm{B}}_{\mathrm{F}}\mathbf{R}^{4} \cdot {}^{\mathrm{F}}\boldsymbol{p}_{\mathrm{H_{org}}} + {}^{\mathrm{B}}\boldsymbol{p}^{4}_{\mathrm{F_{org}}} \end{aligned} \tag{3.18} $$

In order to extract ${}^{\mathrm{F}}\boldsymbol{p}_{\mathrm{H_{org}}}$ from Eq.3.18, we subtract the second to forth equation from the first equation.

$$ \begin{bmatrix} {}^{\mathrm{B}}_{\mathrm{F}}\mathbf{R}^{1} - {}^{\mathrm{B}}_{\mathrm{F}}\mathbf{R}^{2} \\ {}^{\mathrm{B}}_{\mathrm{F}}\mathbf{R}^{1} - {}^{\mathrm{B}}_{\mathrm{F}}\mathbf{R}^{3} \\ {}^{\mathrm{B}}_{\mathrm{F}}\mathbf{R}^{1} - {}^{\mathrm{B}}_{\mathrm{F}}\mathbf{R}^{4} \end{bmatrix} \cdot {}^{\mathrm{F}}\boldsymbol{p}_{\mathrm{H_{org}}} = \begin{bmatrix} {}^{\mathrm{B}}\boldsymbol{p}^{2}_{\mathrm{F_{org}}} - {}^{\mathrm{B}}\boldsymbol{p}^{1}_{\mathrm{F_{org}}} \\ {}^{\mathrm{B}}\boldsymbol{p}^{3}_{\mathrm{F_{org}}} - {}^{\mathrm{B}}\boldsymbol{p}^{1}_{\mathrm{F_{org}}} \\ {}^{\mathrm{B}}\boldsymbol{p}^{4}_{\mathrm{F_{org}}} - {}^{\mathrm{B}}\boldsymbol{p}^{1}_{\mathrm{F_{org}}} \end{bmatrix} \tag{3.19} $$

where

$$ \mathbf{R} = \begin{bmatrix} {}^{\mathrm{B}}_{\mathrm{F}}\mathbf{R}^{1} - {}^{\mathrm{B}}_{\mathrm{F}}\mathbf{R}^{2} \\ {}^{\mathrm{B}}_{\mathrm{F}}\mathbf{R}^{1} - {}^{\mathrm{B}}_{\mathrm{F}}\mathbf{R}^{3} \\ {}^{\mathrm{B}}_{\mathrm{F}}\mathbf{R}^{1} - {}^{\mathrm{B}}_{\mathrm{F}}\mathbf{R}^{4} \end{bmatrix}_{9\times 3}, \mathbf{P} = \begin{bmatrix} {}^{\mathrm{B}}\boldsymbol{p}^{2}_{\mathrm{F_{org}}} - {}^{\mathrm{B}}\boldsymbol{p}^{1}_{\mathrm{F_{org}}} \\ {}^{\mathrm{B}}\boldsymbol{p}^{3}_{\mathrm{F_{org}}} - {}^{\mathrm{B}}\boldsymbol{p}^{1}_{\mathrm{F_{org}}} \\ {}^{\mathrm{B}}\boldsymbol{p}^{4}_{\mathrm{F_{org}}} - {}^{\mathrm{B}}\boldsymbol{p}^{1}_{\mathrm{F_{org}}} \end{bmatrix}_{9\times 1} $$

Therefore,

$$
\begin{aligned}
{}^{\mathrm{F}}\boldsymbol{p}_{\mathrm{H_{org}}} &= \mathbf{R}^{\dagger} \cdot \mathbf{P} \\
&= \left(\mathbf{R}^{\top}\mathbf{R}\right)^{-1} \cdot \mathbf{R}^{\top} \cdot \mathbf{P}
\end{aligned}
$$

Hence, we can utilize four-points method to obtain the translation vector.

3.4.2 Rotation Information

Turning now to the discussion about the rotation vector. In the first place, we have to find the vector of tool insertion direction $\boldsymbol{t}$. By means of TCP method, we can obtain the translation vector from the origin of frame$\{6\}$ to the tool tip. Therefore we use two root canal files with different lengths and apply TCP method to separately obtain two vector illustrated as Fig . Hence,

$$
\boldsymbol{t} = {}^{\mathrm{F}}\boldsymbol{p}_{\mathrm{H_{org,long}}} - {}^{\mathrm{F}}\boldsymbol{p}_{\mathrm{H_{org,short}}} \tag{3.20}
$$

For analyze it easily, we depict it in Fig 3.2. Note that here we only discuss rotation. Because we hope to send z axis command to achieve tool insertion, we should

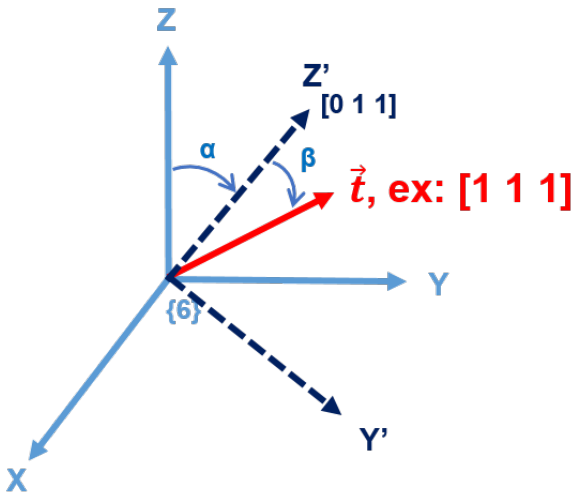

Figure 3.2: Illustration of finding rotation matrix

align original Z axis to the target vector. Therefore, Z axis alignment without other

restrictions will produce many solutions. We choose one of solutions to align Z axis to the target vector. According to the figure, we assume the target vector $\boldsymbol{t}$ is $[x, y, z]$, whose projection to yz-plane $\text{proj}_{(\text{y-z})}\boldsymbol{t}$ is $[0, y, z]$. First, we rotate α degree around X axis to make original Z axis align the projection $[0, y, z]$. Next, we rotate β degree around Y' axis and finally align original Z axis to the target vector [1,1,1]. The following equation

$$
{}^{\text{T}}_{6}\mathbf{R} = \mathbf{R}_{\mathbf{x}}(\alpha) \cdot \mathbf{R}_{\mathbf{y}}(\beta) \tag{3.21}
$$

where

$$
\begin{aligned}
\alpha &= \text{sign}(t_y) \cdot \cos^{-1}\left(\frac{\hat{k} \cdot \text{proj}_{(\text{y-z})}\boldsymbol{t}}{\left\|\hat{k}\right\| \cdot \left\|\text{proj}_{(\text{y-z})}\boldsymbol{t}\right\|}\right) \\
\beta &= \text{sign}(t_x) \cdot \cos^{-1}\left(\frac{\mathbf{t} \cdot \text{proj}_{(\text{y-z})}\boldsymbol{t}}{\|\mathbf{t}\| \cdot \left\|\text{proj}_{(\text{y-z})}\boldsymbol{t}\right\|}\right)
\end{aligned} \tag{3.22}
$$

Assume $\boldsymbol{t} = [x, y, z]$,

$$
\begin{aligned}
\alpha &= \text{sign}(y) \cdot \cos^{-1}\left(\frac{z^2}{\sqrt{y^2 + z^2}}\right) \text{rad} \\
\beta &= \text{sign}(x) \cdot \cos^{-1}\left(\frac{y^2 + z^2}{\sqrt{x^2 + y^2 + z^2}\sqrt{x^2 + y^2 + z^2}}\right) \text{rad}
\end{aligned} \tag{3.23}
$$

α and β are Euler angles, which meet the command demand.

In this section, we have demonstrated two key aspects of reference frame changing of the robot arm. It's easy to input the results of section 3.4.1 and section 3.4.2 via the command setTRF, the robot arm will recognize frame{T}. Having discussed how to combine a robot arm with an end effector, the next section addresses ways of combining an F/T sensor.

Chapter 4

Force-Guided Robot Alignment

This chapter follows on from the previous chapter, we continue to demonstrate some technical solutions of system integration. On top of that, F/T sensor will be included to discuss. Therefore, you can see the chapter as a operating manual when you simultaneously own a robot arm, an F/T sensor and an end effector. First of all, we explain why we will use F/T sensor in our project in section 4.1. Furthermore, we introduce how to do gravity compensation in senction 4.2. Admittance control based on F/T sensor is described in section 4.3.1. Reference Frame Changing of F/T sensor is explained in section 4.4.1. And finally we discuss affection of setting admittance control parameters in section 4.5.

4.1 Problem Definition

(Main cause of surgical failure) (Peg in hole method based on F/T feedback) (Modes: Doctor Dragging and self-alignment) how to compensate the gravity affection in section 4.2; how to use admittance control in section with F/T sensor 4.3.1; and how to obtain the real force and torque values in the tool tip frame in section 4.4.1

4.2 Integration of F/T sensor

Gravity compensation is a standard technical issue when combining an F/T sensor, a robot arm and an end effector.

4.3 Alignment to the Root Canal (Dragging for alignment)

4.3.1 Admittance Control based on F/T sensor

Admittance control make the robot move like a spring-mass-damper system. Forces and torques can be mapped into the movements such as position or velocity. Therefore, Admittance control allows an robot arm to cooperate with human in a safe work environment. In this section we propose a control scheme depicted as Figure 4.1. Since Meca500 is an industrial robot arm without admittance control, we

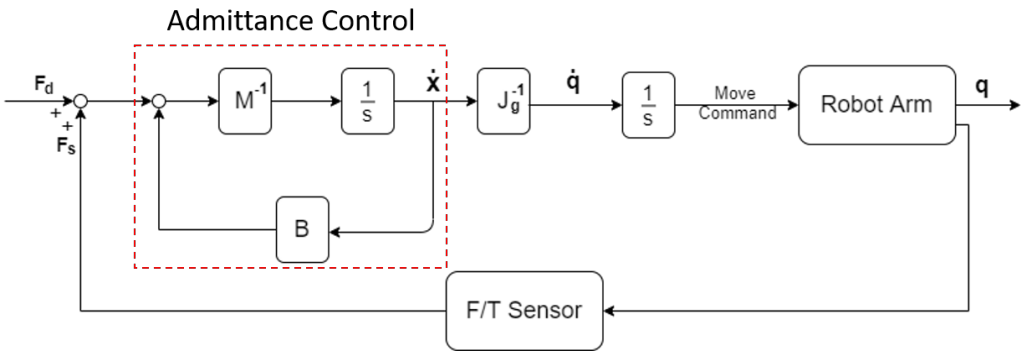

Figure 4.1: Control scheme. Where F_d denotes the desired forces and torques vector. F_s denotes the real value detected by F/T sensor and is also a forces and torques vector. $\dot{\mathbf{x}}$ denotes $[\dot{x}, \dot{y}, \dot{z}, \dot{\theta}_x, \dot{\theta}_y, \dot{\theta}_z]$. J_g denotes the geometric Jacobian matrix. $\dot{\mathbf{q}}$ denotes $[\dot{\theta}_1, \dot{\theta}_2, \dot{\theta}_3, \dot{\theta}_4, \dot{\theta}_5, \dot{\theta}_6]$. $\mathbf{q}$ denotes $[\theta_1, \theta_2, \theta_3, \theta_4, \theta_5, \theta_6]$

combine the robot arm with the F/T sensor to enable admittance control. With force and torque feedback, F/T sensor make Meca500 like a cooperative robot arm.

It's worth noting that in this approach the admittance control function is triggered by the end effector mounted on F/T sensor instead of each wrist of the robot arm.

$$\begin{bmatrix} x \\ y \\ z \\ \theta_x \\ \theta_y \\ \theta_z \end{bmatrix} = \frac{1}{MS^2 + BS + K} \begin{bmatrix} f_x \\ f_y \\ f_z \\ \tau x \\ \tau y \\ \tau z \end{bmatrix} \tag{4.1}$$

where M,B,K are diagonal positive definite matrices. Affections of these parameters will be discussed in next section.

A standard equation of admittance control is represented as Eq 4.1. The values we obtain from the F/T sensor are $[f_x, f_y, f_z, \tau_x, \tau_y, \tau_z]$, whose forces $[f_x, f_y, f_z]$ are related to the translations $[x, y, z]$ and torques $[\tau_x, \tau_y, \tau_z]$ are related to the axis angle $[\theta_x, \theta_y, \theta_z]$. In our approach we ignore parameter K which is relevant to spring stiffness because our system should behave like a mass-damper system. Bounce similar to a spring is not necessary in whole project.

There are few commands of moving the robot arm. Such as position command MoveJoints($\theta_1, \theta_2, \theta_3, \theta_4, \theta_5, \theta_6$)and MovePose(x,y,z,$\alpha$ β γ); velocity command MoveJointsVel

4.4 Alignment to the Root Canal (Drilling and self-alignment)

4.4.1 Reference Frame Changing of F/T sensor

(Transformation from robot to tool [Chapt. 3.4]+ Transformation from sensor to tool) (How to find the direction vector of the tool) (From sensor frame to tool tip frame)

4.4.2 Motion Planning: Based on Admittance Control

(Block diagram, robot command choice)

4.5 Discussion about Affection of Parameter Setting

(K, Bi, Mi- without numbers) (Modes: Doctor Dragging and Self-alignment - with numbers; get reasonable and suitable parameters first)

Chapter 5

Control of Endodontic File Rotation

5.1 Problem Definition

(Main cause of Files Fracture)

(File property)

5.2 The Proposed Method and Theorem

Weak section! add some technical solutions (CACS2020)(Prototype 1)

(Motion Planning: sections)(Current threshold setting)

Chapter 6

Preliminary Experiment Result

6.1 Experimental Setup

(Communication protocol – EtherCAT, RTOS – NI target)

For 6.2 experiment: (Stewart-Platform + PhaseSpace + markers)

For 6.3 6.4 experiments: (Acrylic root canal model + truth tooth)

6.2 Admittance Control

(Metrics: position comparison between the target and the robot)

6.3 Automatically Direction Changing

(Metrics: time, completeness and file breakage)

(Completeness definition: comparison of pixel area before and after experiment via image)

6.4 Repetitive Experiment

(Metrics: file breakage, compare with and without reverse)

Chapter 7

Conclusions and Future works

(Patient move tracking via cable, root canals searching)

Chapter 8

Appendix

8.1 Forward Kinematics

$$
{}^0_6\mathrm{T} = {}^0_1\mathrm{T} \cdot {}^1_2\mathrm{T} \cdot {}^2_3\mathrm{T} \cdot {}^3_4\mathrm{T} \cdot {}^4_5\mathrm{T} \cdot {}^5_6\mathrm{T} = \begin{bmatrix} {}^0_6\mathrm{R}_{3\times3} & {}^0\vec{P}_{6org} \\ 0_{1\times3} & 1 \end{bmatrix} = \begin{bmatrix} {}^0_6\mathrm{T}_{00} & {}^0_6\mathrm{T}_{01} & {}^0_6\mathrm{T}_{02} & {}^0_6\mathrm{T}_{03} \\ {}^0_6\mathrm{T}_{10} & {}^0_6\mathrm{T}_{11} & {}^0_6\mathrm{T}_{12} & {}^0_6\mathrm{T}_{13} \\ {}^0_6\mathrm{T}_{20} & {}^0_6\mathrm{T}_{21} & {}^0_6\mathrm{T}_{22} & {}^0_6\mathrm{T}_{23} \\ 0 & 0 & 0 & 1 \end{bmatrix}
$$

$$
\begin{aligned}
{}^0_6\mathbf{T}_{00} =& - S_6(C_4S_1 + S_4(C_1S_3 - C_2 - C_1C_3S_2)) - C_6(C_5(S_1S_4 - C_4(C_1S_3 - C_2 - C_1C_3S_2)) \\
& - S_5(C_1C_3 - C_2 + C_1S_2S_3)) \\
{}^0_6\mathrm{T}_{01} =& S_6(C_5(S_1S_4 - C_4(C_1S_3 - C_2 - C_1C_3S_2)) - S_5(C_1C_3 - C_2 + C_1S_2S_3)) - C_6(C_4S_1 \\
& + S_4(C_1S_3 - C_2 - C_1C_3S_2)) \\
{}^0_6\mathrm{T}_{02} =& - S_5(S_1S_4 - C_4(C_1S_3 - C_2 - C_1C_3S_2)) - C_5(C_1C_3 - C_2 + C_1S_2S_3) \\
{}^0_6\mathrm{T}_{03} =& 135C_1S_2 - 70S_5(S_1S_4 - C_4(C_1S_3 - C_2 - C_1C_3S_2)) - 70C_5(C_1C_3 - C_2 + C_1S_2S_3) \\
& - 120C_1C_3 - C_2 - 120C_1S_2S_3 - 38C_1S_3 - C_2 + 38C_1C_3S_2 \\
{}^0_6\mathrm{T}_{10} =& S_6(C_1C_4 + S_4(C_3S_2S_1 - S_1S_3 - C_2)) + C_6(C_5(C_1S_4 - C_4(C_3S_2S_1 - S_1S_3 - C_2)) \\
& + S_5(C_3S_1 - C_2 + S_2S_1S_3)) \\
{}^0_6\mathrm{T}_{11} =& C_6(C_1C_4 + S_4(C_3S_2S_1 - S_1S_3 - C_2)) - S_6(C_5(C_1S_4 - C_4(C_3S_2S_1 - S_1S_3 - C_2)) \\
& + S_5(C_3S_1 - C_2 + S_2S_1S_3)) \\
{}^0_6\mathrm{T}_{12} =& S_5(C_1S_4 - C_4(C_3S_2S_1 - S_1S_3 - C_2)) - C_5(C_3S_1 - C_2 + S_2S_1S_3) \\
{}^0_6\mathrm{T}_{13} =& 135S_2S_1 + 70S_5(C_1S_4 - C_4(C_3S_2S_1 - S_1S_3 - C_2)) - 70C_5(C_3S_1 - C_2 + S_2S_1S_3) \\
& + 38C_3S_2S_1 - 120C_3S_1 - C_2 - 120S_2S_1S_3 - 38S_1S_3 - C_2 \\
{}^0_6\mathrm{T}_{20} =& C_6(S_5(C_3S_2 - S_3 - C_2) + C_4C_5(C_3 - C_2 + S_2S_3)) - S_4S_6(C_3 - C_2 + S_2S_3) \\
{}^0_6\mathrm{T}_{21} =& - S_6(S_5(C_3S_2 - S_3 - C_2) + C_4C_5(C_3 - C_2 + S_2S_3)) - C_6S_4(C_3 - C_2 + S_2S_3) \\
{}^0_6\mathrm{T}_{22} =& C_4S_5(C_3 - C_2 + S_2S_3) - C_5(C_3S_2 - S_3 - C_2) \\
{}^0_6\mathrm{T}_{23} =& 120S_3 - C_2 - 120C_3S_2 - 38C_3 - C_2 - 38S_2S_3 - 135 - C_2 - 70C_5(C_3S_2 - S_3 - C_2) \\
& + 70C_4S_5(C_3 - C_2 + S_2S_3) + 135
\end{aligned}
$$

8.2 Jacobian matrix

$$J_{g0,00} = 120S_1S_2S_3 - 38C_2S_1S_3 - 38C_3S_1S_2 - 70C_1S_4S_5 - 135S_1S_2 - 120C_2C_3S_1 - 70C_2C_3C_5S_1 + 70C_5S_1S_2S_3 + 70C_2C_4S_1S_3S_5 + 70C_3C_4S_1S_2S_5$$

$$J_{g0,01} = -C_1(120C_2S_3 - 38C_2C_3 - 135C_2 + 120C_3S_2 + 38S_2S_3 + 70C_2C_5S_3 + 70C_3C_5S_2 + 70C_2C_3C_4S_5 - 70C_4S_2S_3S_5)$$

$$J_{g0,02} = -2C_1(60C_2S_3 - 19C_2C_3 + 60C_3S_2 + 19S_2S_3 + 35C_2C_5S_3 + 35C_3C_5S_2 + 35C_2C_3C_4S_5 - 35C_4S_2S_3S_5)$$

$$J_{g0,03} = 70S_5(C_1C_2S_3S_4 - C_4S_1 + C_1C_3S_2S_4)$$

$$J_{g0,04} = -70C_5(S_1S_4 + C_1C_2C_4S_3 + C_1C_3C_4S_2) - 70C_{23}C_1S_5$$

$$J_{g0,05} = 0$$

$$J_{g0,10} = 135C_1S_2 - 120C_1S_2S_3 - 70S_1S_4S_5 + 120C_1C_2C_3 + 38C_1C_2S_3 + 38C_1C_3S_2 + 70C_1C_2C_3C_5 - 70C_1C_5S_2S_3 - 70C_1C_2C_4S_3S_5 - 70C_1C_3C_4S_2S_5$$

$$J_{g0,11} = -S_1(120C_2S_3 - 38C_2C_3 - 135C_2 + 120C_3S_2 + 38S_2S_3 + 70C_2C_5S_3 + 70C_3C_5S_2 + 70C_2C_3C_4S_5 - 70C_4S_2S_3S_5)$$

$$J_{g0,12} = -2S_1(60C_2S_3 - 19C_2C_3 + 60C_3S_2 + 19S_2S_3 + 35C_2C_5S_3 + 35C_3C_5S_2 + 35C_2C_3C_4S_5 - 35C_4S_2S_3S_5)$$

$$J_{g0,13} = 70S_5(C_1C_4 + C_2S_1S_3S_4 + C_3S_1S_2S_4)$$

$$J_{g0,14} = -70C_5(C_2C_4S_1S_3 - C_1S_4 + C_3C_4S_1S_2) - 70C_{23}S_1S_5$$

$$J_{g0,15} = 0$$

$$J_{g0,20} = 0$$

$$J_{g0,21} = 120S_2S_3 - 120C_2C_3 - 38C_2S_3 - 38C_3S_2 - 135S_2 + 70C_5S_2S_3 - 70C_2C_3C_5 + 70C_2C_4S_3S_5 + 70C_3C_4S_2S_5$$

$$J_{g0,22} = 120S_2S_3 - 38C_2S_3 - 38C_3S_2 - 120C_2C_3 + 70C_5S_2S_3 - 70C_2C_3C_5 + 70C_2C_4S_3S_5 + 70C_3C_4S_2S_5$$

$$J_{g0,23} = 70C_{23}S_4S_5$$

$$J_{g0,24} = 70S_{23}S_5 - 70C_{23}C_4C_5$$

$$J_{g0,25} = 0$$

$$J_{g0,30} = \theta_4S_1S_2S_3 - \theta_3C_1 - \theta_5C_1C_4 - \theta_4C_2C_3S_1 - \theta_6C_1S_4S_5 - \theta_2C_1 - \theta_6C_2C_3C_5S_1 - \theta_5C_2S_1S_3S_4 - \theta_5C_3S_1S_2S_4 + \theta_6C_5S_1S_2S_3 + \theta_6C_2C_4S_1S_3S_5 + \theta_6C_3C_4S_1S_2S_5$$

$$J_{g0,31} = \theta_5C_1C_2C_3S_4 - \theta_4C_1C_2S_3 - \theta_4C_1C_3S_2 - S_1 - \theta_6C_1C_2C_5S_3 - \theta_6C_1C_3C_5S_2$$

$$J_{g0,40} = \theta_4 C_1 C_2 C_3 - \theta_3 S_1 - \theta_5 C_4 S_1 - theta2 S_1 - \theta_4 C_1 S_2 S_3 - \theta_6 S_1 S_4 S_5 + \theta_6 C_1 C_2 C_3 C_5$$
$$+ \theta_5 C_1 C_2 S_3 S_4 + \theta_5 C_1 C_3 S_2 S_4 - \theta_6 C_1 C_5 S_2 S_3 - \theta_6 C_1 C_2 C_4 S_3 S_5 - \theta_6 C_1 C_3 C_4 S_2 S_5$$

$$J_{g0,41} = C_1 - \theta_4 C_2 S_1 S_3 - \theta_4 C_3 S_1 S_2 + \theta_5 C_2 C_3 S_1 S_4 - \theta_6 C_2 C_5 S_1 S_3 - \theta_6 C_3 C_5 S_1 S_2$$
$$- \theta_5 S_1 S_2 S_3 S_4 - \theta_6 C_2 C_3 C_4 S_1 S_5 + \theta_6 C_4 S_1 S_2 S_3 S_5$$

$$J_{g0,42} = C_1 - \theta_4 C_2 S_1 S_3 - \theta_4 C_3 S_1 S_2 + \theta_5 C_2 C_3 S_1 S_4 - \theta_6 C_2 C_5 S_1 S_3 - \theta_6 C_3 C_5 S_1 S_2$$
$$- \theta_5 S_1 S_2 S_3 S_4$$
$$- \theta_6 C_2 C_3 C_4 S_1 S_5 + \theta_6 C_4 S_1 S_2 S_3 S_5$$

$$J_{g0,43} = \theta_5 (C_2 C_4 S_1 S_3 - C_1 S_4 + C_3 C_4 S_1 S_2) + \theta_6 S_5 (C_1 C_4 + C_2 S_1 S_3 S_4 + C_3 S_1 S_2 S_4)$$
$$- S_1 S_2 S_3 + C_2 C_3 S_1$$

$$J_{g0,44} = C_1 C_4 + S_{23} S_1 S_4 - \theta_6 C_{23} S_1 S_5 + \theta_6 C_1 C_5 S_4 - \theta_6 C_2 C_4 C_5 S_1 S_3 - \theta_6 C_3 C_4 C_5 S_1 S_2$$

$$J_{g0,45} = C_{23} C_5 S_1 - S_5 (C_2 C_4 S_1 S_3 - C_1 S_4 + C_3 C_4 S_1 S_2)$$

$$J_{g0,50} = 1$$

$$J_{g0,51} = \theta_6 S_{23} C_4 S_5 - \theta_6 C_{23} C_5 - \theta_5 S_{23} S_4 - \theta_4 C_{23}$$

$$J_{g0,52} = \theta_6 S_{23} C_4 S_5 - \theta_6 C_{23} C_5 - \theta_5 S_{23} S_4 - \theta_4 C_{23}$$

$$J_{g0,53} = \theta_5 C_2 C_3 C_4 - C_3 S_2 - C_2 S_3 - \theta_5 C_4 S_2 S_3 + \theta_6 C_2 C_3 S_4 S_5 - \theta_6 S_2 S_3 S_4 S_5$$

$$J_{g0,54} = \theta_6 (S_{23} S_5 - C_{23} C_4 C_5) + C_{23} S_4$$

$$J_{g0,55} = - S_{23} C_5 - C_{23} C_4 S_5$$

$$J_{g6,00} = 135 C_4 S_2 S_6 + 120 C_2 C_3 C_4 S_6 + 70 C_2 C_3 C_6 S_4 + 38 C_2 C_4 S_3 S_6 + 38 C_3 C_4 S_2 S_6$$
$$+ 135 C_5 C_6 S_2 S_4 - 120 C_4 S_2 S_3 S_6 - 70 C_6 S_2 S_3 S_4 - 70 C_2 S_3 S_5 S_6 - 70 C_3 S_2 S_5 S_6$$
$$+ 70 C_2 C_3 C_4 C_5 S_6 + 120 C_2 C_3 C_5 C_6 S_4 + 38 C_2 C_5 C_6 S_3 S_4 + 38 C_3 C_5 C_6 S_2 S_4$$
$$- 70 C_4 C_5 S_2 S_3 S_6 - 120 C_5 C_6 S_2 S_3 S_4$$

$$J_{g6,01} = 70 C_4 C_6 - 38 C_6 S_5 - 120 S_4 S_6 - 70 C_5 S_4 S_6 + 135 S_3 S_4 S_6 + 120 C_4 C_5 C_6 - 135 C_3 C_6 S_5$$
$$- 135 C_4 C_5 C_6 S_3$$

$$J_{g6,02} = 70 C_4 C_6 - 38 C_6 S_5 - 120 S_4 S_6 - 70 C_5 S_4 S_6 + 120 C_4 C_5 C_6$$

$$J_{g6,03} = 70 S_5 S_6$$

$$J_{g6,04} = 70 C_6$$

$$J_{g6,05} = 0$$

$$J_{g6,10} = 135 C_4 C_6 S_2 + 120 C_2 C_3 C_4 C_6 + 38 C_2 C_4 C_6 S_3 + 38 C_3 C_4 C_6 S_2 - 70 C_2 C_3 S_4 S_6$$
$$- 120 C_4 C_6 S_2 S_3 - 70 C_2 C_6 S_3 S_5 - 70 C_3 C_6 S_2 S_5 - 135 C_5 S_2 S_4 S_6 + 70 S_2 S_3 S_4 S_6$$
$$+ 70 C_2 C_3 C_4 C_5 C_6 - 120 C_2 C_3 C_5 S_4 S_6 - 70 C_4 C_5 C_6 S_2 S_3 - 38 C_2 C_5 S_3 S_4 S_6$$

Reference

[1] C. Yang, J. Wang, L. Mi, X. Liu, Y. Xia, Y. Li, S. Ma, and Q. Teng, "A four-point measurement model for evaluating the pose of industrial robot and its influence factor analysis," *Industrial Robot: An International Journal*, 2017.